Rate Control for Multi-link and Multi-relay Wireless LANs Supporting Real-Time Mobile Data Transmissions

Kazuki Ikeda[1], Shohei Omoto[2], Hiroyuki Yomo[1,2](✉), Yoshihisa Kondo[2], and Hiroyuki Yokoyama[2]

[1] Graduate School of Science and Engineering, Kansai University, Suita, Japan
yomo@kansai-u.ac.jp

[2] ATR Adaptive Communications Research Laboratories, Kyoto, Japan

Abstract. When a wireless LAN station (STA) installed on a mobile device, such as drone, communicates with an access point (AP) deployed over the ground, its link condition becomes unstable due to mobility and/or interference from surrounding equipment. In this paper, in order to realize reliable data transmissions in such a severe condition, we introduce a multi–link and multi–relay system integrated with broadcast transmissions employing packet–level forward error correction. As a proof–of–concept (PoC), we first conduct an experiment investigating the effectiveness and practicality of the considered multi–link and multi–relay system supporting data transmissions from a drone. Then, we enhance it by proposing rate control for STA to dynamically set its physical layer (PHY) rate based on its position and the link quality for surrounding relays. We also apply overhearing function to each relay to prevent redundant forwarding of the same packets by multiple relays. Our simulation results show an interesting observation that the multi–link and multi–relay system improves energy efficiency of relays when the proposed rate control and overhearing are jointly employed. Furthermore, we show that the multi–link and multi–relay system with link–level broadcast has superior performance to a common unicast based system.

Keywords: Wireless LAN · Drone · Robustness · Real–time data transmissions · Rate control · Relay

1 Introduction

Real–time transmissions of sensing and image/video data from a highly mobile terminal, such as drone, enable many applications such as disaster response,

This work includes results of the project entitled "R&D on Adaptive Media Access Control for Increasing the Capacity of Wireless IoT Devices in Factory Sites," which is supported by the Ministry of Internal Affairs and Communications as part of the research program "R&D for Expansion of Radio Wave Resources (JPJ000254)".

T. Hara and H. Yamaguchi (Eds.): MobiQuitous 2021, LNICST 419, pp. 707–723, 2022.
https://doi.org/10.1007/978-3-030-94822-1_46

environmental monitoring, infrastructure management, live event streaming, etc. [1,2]. In this paper, we focus on real–time data transmissions from a drone supported by wireless LAN (WLAN). The most common communication mode in WLAN is a *single–link unicast*: a station (STA) installed on a drone is associated/connected to a single access point (AP) deployed over the ground. However, data transmissions with a single AP are vulnerable to link disconnections due to interference and mobility of drone [3]. In order to overcome this problem, in our previous work, we advocated exploiting multiple reception points offered by multiple APs deployed over the ground [4]. Each data is transmitted by STA with link–level broadcast such that route diversity through multiple reception points is exploited while its reliability is enhanced by applying packet–level forward error correction. However, the deployment of multiple APs, which requires wired connections to a gateway (GW), increases its system cost, and also limits its flexibility to change the configuration of reception points. In order to solve this problem, in this paper, we introduce multiple relays into our system setting. The multiple reception points are realized by battery–operated, portable wireless relays, which can provide flexibility for their deployment. Furthermore, we also apply multi–link transmissions in order to enjoy channel diversity for WLAN transmissions. Since WLAN utilizes the unlicensed frequency band, an operating channel can suffer from severe interference caused by surrounding radio equipment. With multi–link transmissions over multiple operating channels, even if one channel is highly occupied by the interfering unlicensed devises, the other channel can be free of interference, which can enhance the robustness in highly–interfered scenarios.

An important parameter to be tuned in our system setting described above is physical layer (PHY) rate employed by STA. A smaller PHY rate increases the number of relays, to which STA can deliver data, thereby improving the spatial reliability. However, the duration of packet transmission is increased with the smaller PHY rate, which increases the airtime (i.e., channel occupancy period) and gives negative impact on the other radio equipment sharing the same channel. A common approach to PHY rate adaptation in WLAN is the rate control based on feedback (i.e., ACK) returned from a possible receiver. However, the system considered in this paper employs link–level broadcast by STA, which in general is difficult to employ ACK and retransmission mechanisms. Due to this difficulty, IEEE 802.11, which is employed for PHY and medium access control (MAC) protocol of WLAN in this paper, does not implement ACK for link–level broadcast. Therefore, we need to design rate control that does not count on feedback from receivers. Furthermore, high mobility of drone does not allow STA to spend sufficiently long time to decide its optimal PHY rate at each position. Therefore, it is necessary to design rate control that can promptly decide PHY rate to be employed at a given position of drone.

In this paper, as a proof–of–concept (PoC), we first conduct an experiment investigating the effectiveness and practicality of the considered multi–link and multi–relay system supporting data transmissions from a drone. Then, we enhance it by proposing a rate control for WLAN STA installed on drone, which promptly decides PHY rate to be employed at a given position based on its link conditions for surrounding relays without resorting to ACK. The proposed rate control introduces a calibration phase before system operations, during which the drone conducts test flight over the given communication area and preliminary observes the radio environment. Specifically, the drone transmits probing signals at different positions over the given area, with which each relay measures the received signal strength and forwards them to an AP. Based on the received/observed information, AP constructs a mapping table between different positions over the area and PHY rates to be employed, which is then set to STA. During the system operations, STA on drone decides its PHY rate based on its position and given mapping table. We also apply overhearing function to each relay in order to prevent redundant forwarding of the same packets by multiple relays. With computer simulations, we evaluate performance of multi–link and multi–relay transmissions with the proposed rate control in terms of packet delivery rate, delay, airtime, and energy consumption of wireless relays, and investigate the effectiveness of the proposed rate control as well as multi–link/multi–relay configurations.

Some existing work focus on the video streaming from drone to a ground station. For instance, video rate adaptation is investigated for adapting to variable air–to–ground channel in [1,2]. The PHY rate adaptation based on sensor state of unmanned aerial vehicle (UAV) is proposed in [3]. While these work focus on direct transmissions of video from drone to a ground station, the use of relay with routing protocols is also considered, e.g., in [5]. Unlike these work, our work introduces multi–link relaying combined with link–level broadcast and packet–level FEC into data transmissions from drone, for which PHY rate adaptation is proposed to take trade–off between reliability and efficiency.

2 System Model

The system model considered in this paper is shown in Fig. 1. A single AP, which is connected to a gateway (GW) through a wired connection, is deployed over a target communication area together with multiple relaying nodes (RNs). A drone flies over the communication area, and its onboard STA attempts to transmit data to GW through RNs and AP. We assume that GPS module is installed on the drone to identify its position. The STA is equipped with multiple WLAN IFs operating over different channels, which are used for multi–link data transfer. When multiple drones (i.e., STAs) are considered, the same set of channels can be allocated and shared by different STAs. Therefore, the number of required channels is not dependent on the number of considered drones. On the other hand, the number of WLAN IFs owned by each RN is assumed to be $N_{RN} = N_{STA} + N_F$, where N_{STA} is the number of IFs used by STA for multi–link transmissions and N_F is that employed by RN for data forwarding to AP. The number of IFs installed into AP, N_{AP}, is supposed to be sufficient to receive data transmitted by STA and/or RS over any channel. All the WLAN IFs are assumed to follow IEEE 802.11n protocols. The example in Fig. 1 shows the case with $N_{STA} = 2$, $N_F = 1$, and $N_{AP} = 4$, where different channels are assigned to separate IFs for data transmissions/forwarding by STA/RNs. This multi–link/multi–channel configuration allows us to exploit *channel diversity*: even if some channels are severely interfered by many unlicensed equipment, data transmitted by the other channels with less interference can be successfully delivered with high probability. Furthermore, in order to exploit multiple reception points realized by RNs, STA employs link–level broadcast combined with packet–level forward error correction (FEC). In this scheme, for a batch of K data packets to be transfered to GW, STA transmits $N = K + M$ packets at each IF, where M packets are redundant packets generated from K data packets by using random linear network coding (RLNC) [6]. At GW, if any set of K packets out of $N = K + N_{STA}M$ packets are successfully received, it can recover the original K data packets. This enables us to enjoy *route diversity*: GW can recover packets lost over a route between STA and GW from the other packets successfully received over the separate routes, thereby enhancing the reliability of mobile data transmissions.

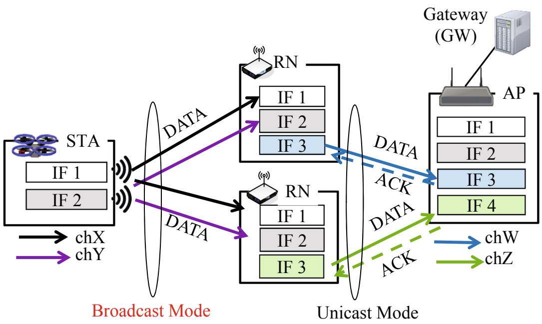

Fig. 1. Considered multi–link and multi–relay data transmission system.

On the other hand, we employ standard unicast transmissions for data forwarding from RNs to AP, considering that RNs and AP are static nodes. Each IF at RN for data forwarding is connected to an IF at AP, where retransmission mechanisms based on ACK exchange and dynamic rate control with automatic rate fallback (ARF) [7] are employed.

3 An Experiment on Multi–link and Multi–relay Transmissions from a Drone

As PoC of the multi–link and multi–relay system supporting data transmissions from a drone, we conducted an experiment to investigate its effectiveness and practicality. The experimental setting is shown in Fig. 2. The experiment was conducted at a test field set up by JUIDA [8]. The STA installed on a drone

(DJI phantom 4 [9]) and each RN are realized by Raspberry Pi 3 model B+ with commercial, off–the–shelf WLAN USB dongles. On the other hand, AP consists of a Raspberry Pi 3 model B+ and an off–the–shelf WLAN router. A laptop PC is used to aggregate data packets transmitted by STA through RNs. The drone with STA on board repeatedly flies over the test field with the height of 10m as shown in Fig. 2.

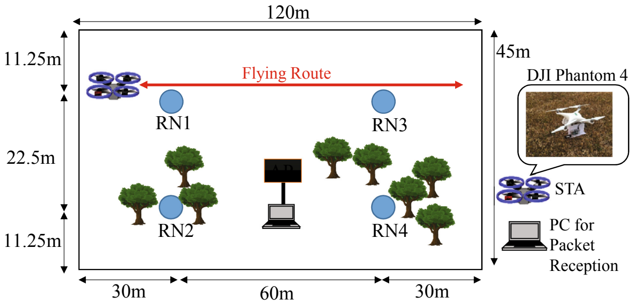

Fig. 2. Experimental settings of multi–link and multi–relay data transmissions from a drone.

Two WLAN USB dongles are inserted into the Raspberry Pi of STA, whose channels are set to different channels over 2.4 GHz band. For a regulatory reason, we employed 2.4 GHz for data transmissions from STA on drone. Similarly, two WLAN USB dongles set to operate over the corresponding 2.4 GHz channels are put into the Raspberry Pi of RN. Furthermore, an internal WLAN IF of the Raspberry Pi of RN is used to forward data packets to the WLAN router in AP, which uses a single channel over 5 GHz. The Raspberry Pi in AP also has two WLAN USB dongles to directly receive data from STA. That is, we have a configuration with $N_{STA} = 2$, $N_F = 1$, $N_{RN} = 3$, and $N_{AP} = 3$. For multi–link transmissions from STA, the same set of packets are transmitted with link–level broadcast over each IF, where its FEC rate is fixed to be 1/2 ($K = 10$). The number of RNs is assumed to be 4 as shown in Fig. 2. These RNs are controlled to forward all packets successfully received from STA to AP with unicast mode, where PHY rate control implemented into the employed USB dongle by default is activated. The packets with their size of 1400 Bytes are transmitted with the interval of 10 ms, where the total number of data packets transmitted is fixed to be 6000.

In the experiment, we evaluated application–level packet delivery rate (PDR) (i.e., PDR after FEC decoding) and airtime per IF at STA for the transmissions employing multi–link and multi–relay broadcast explained in Sect. 2 (called ML–BC hereafter) and those activating only a single IF at STA, i.e., single–link and multi–relay broadcast (called SL–BC hereafter). Table 1 shows PDR and airtime per IF of ML–BC and SL–BC for different, fixed PHY rates set to STA. From this table, we can first see that PDR is improved by employing lower PHY rate. Specifically, by employing 14.4 Mbps as PHY rate at STA, PDR of 100% is achieved even for SL–BC. This is because smaller signal–to–noise ratio (SNR) is sufficient for packets transmitted with lower PHY rate to be received successfully at reception points, which however sacrifices airtime as observed in Table 1. In order to reduce airtime, it is preferred to employ higher PHY rate, however, SL–BC cannot offer PDR of 100% for PHY rate of 86.7 Mbps while it is possible with ML–BC. Furthermore, ML–BC largely improves PDR in comparison to SL–BC for PHY rate of 144 Mbps. This is thanks to channel diversity: even if a packet transmitted over one IF is lost due to low SNR or high interference, it can be delivered to a reception point successfully over the other IF. These experimental results and our implementation of multi–link and multi–relay system confirm its effectiveness and practicality.

Table 1. Experimental Results

	PDR [%]	Airtime per IF at STA [s]
SL–BC (14.4 Mbps)	100	10.25
SL–BC (86.7 Mbps)	98.37	2.12
SL–BC (144 Mbps)	63.77	1.48
ML–BC (14.4 Mbps)	100	10.25
ML–BC (86.7 Mbps)	100	2.12
ML–BC (144 Mbps)	83.33	1.48

4 Enhancements to Multi–link and Multi–relay System

In this work, we enhance the multi–link and multi–relay system supporting data transmissions from a drone by two mechanisms: PHY rate control and overhearing. While overhearing is a well-known approach for wireless relaying [10] to select a best relay, there is no PHY rate control specific to multi–link and multi–relay system with link–level broadcast. Therefore, we newly propose a rate control mechanism explained below.

4.1 PHY Rate Control

In this paper, we propose a PHY rate control for WLAN STA on drone, which can cope with the rapid change of link qualities to surrounding RNs. We first divide the communication area into several grids, and STA decides its PHY rate to be employed according to its staying grid. The PHY rate to be employed in each grid is decided based on *test flight*, which is carried out just before its operations over the corresponding communication area. This kind of pre–measurement regarding connectivity/coverage is commonly employed for optimizing parameters at a given communication area, which is employed for PHY rate adaptation in this work. During test flight, the drone moves to the center of each grid and transmits control packets, which are then used by AP to decide the best rate at each grid. The decision on PHY rate consists of the following 2 steps:

Step 1: The objective of this step is to extract the average received signal strength indicators (RSSIs) between each IF at STA and surrounding RNs. The STA broadcasts packets including its GPS information (i.e., its location) from each IF at the center of each grid for a given period of time. Then, each RN forwards the received packets to AP, in which the information on RSSI observed when receiving each packet is added. During test flight, each RN is controlled to forward all received packets to AP. Based on the forwarded packets, AP calculates the average RSSIs between each IF at STA and its surrounding RNs for a given position of STA.

Step 2: In this step, PHY rate to be employed by each IF at STA at each grid is decided by using the information obtained in Step 1. Based on the average RSSIs between an IF and surrounding RNs, packet loss rate (PLR) for each PHY rate is first calculated for each link. To this end, we use Nist Error Rate Model [11]. Here, let us denote the available PHY rate as R_i $(1 \leq i \leq R_{max})$, where R_{max} is the number of available PHY rates. For each R_i, its PLR is calculated as PLR_i. Then, the number of RNs, to which STA is able to deliver its data with $PLR_i \leq PLR_{th}$, is calculated as N_i, where PLR_{th} is a given parameter to control the achieved reliability between each IF at STA and surrounding RNs. Then, PHY rate for a given grid j for an IF X at STA is decided as follows:

$$R_j^X = max\{R_i | N_i \geq N_{min}\}, \tag{1}$$

where N_{min} is the minimum number of RNs, to which STA should deliver data to achieve the required reliability. The basic idea of this decision process is that each STA should select as high rate as possible on condition that it can deliver its data to at least N_{min} RNs with high reliability.

Through the above 2 steps, a mapping table, which maps PHY rate to be employed into each grid ID, is constructed by AP for each IF at STA. This mapping table is notified to STA on drone before the main operations of data transfer over the communication area. During the main operations, STA on drone continuously checks its current position by using GPS information, and decides which grid it is belonging to. Then, by using the given mapping table, STA on drone extracts PHY rate to be employed in a given position, and transfers data with the selected rate. Note that the PHY rate is adapted based on *average* RSSI mainly affected by path loss, which is considered to be static over the operations of drone.

4.2 Overhearing

In addition to the proposed rate control, we employ overhearing (OH) mechanism in order to reduce the probability that the same packets are forwarded by different RNs. With OH mechanism, each RN stores each received packet for a given timer period, which is differently set for each RN. If the timer expires, RN forwards the stored packet to AP. On the other hand, if RN overhears the same packet as the stored one before the timer expires, it cancels the forwarding of the corresponding packet. This enables each RN to avoid redundantly forwarding the same packets to AP, which contributes to the reduction of data traffic as well as power consumption of each RN. The timer for the i–th RN, T_i is decided by AP as follows:

$$T_i = (DIFS + CW_{ave} \times t_s + \frac{B_p}{\gamma_{ave}}) \times \gamma_i. \tag{2}$$

Here, t_s is slot time, B_p is the packet size, and γ_{ave} is the average PHY rate to be employed by RN. Furthermore, CW_{ave} is given by

$$CW_{ave} = \frac{(minCW + 1) \times 2^{maxRN} - 1}{2}, \tag{3}$$

where $minCW$ is the minimum size of contention window and $maxRN$ is the maximum number of retransmissions. The basic idea of Eq. (2) is that each RN should set its timer to the average duration required for data forwarding multiplied by an coefficient γ_i decided based on the quality of link between RN_i and AP. Each RN notifies RSSIs observed over each IF for data forwarding to AP, based on which AP decides γ_i and notifies it to RN_i. For RN with the best link quality, this coefficient is set to 0 while it is increased by 1 for the following RNs with the decreasing order of link quality. With the above OH mechanism, we can increase the probability that each packet is forwarded by a RN with the better link quality to AP. Note that, in order to further reduce the congestion level between RNs and AP, each RN is controlled to forward at most K packets out of successfully received packets for each batch.

5 Numerical Results and Discussions

5.1 Simulation Model

The simulation model and parameters are respectively shown in Fig. 3 and Table 2. A drone installing STA is assumed to move inside the communication area based on Random Way Point model [14]. We assume that 2 IFs at STA operate over different 2.4 GHz channels (i.e., $N_{STA} = 2$) while a single IF at each RN to forward packets to AP employs a single channel over 5 GHz band (i.e., $N_F = 1$). The APs are supposed to have 5 IFs (i.e., $N_{AP} = 5$), 2 IFs with 2.4 GHz band to directly receive packets from STA if possible, and 3 IFs with 5 GHz band for receiving packets forwarded by each RN. Different channels over 5 GHz are allocated to 3 IFs at AP, and each operating channel at RN over 5 GHz is randomly selected. For the proposed rate control, we employ a grid size of 20 m $\times$ 20 m, $N_{min} = 2$, and $PLR_{th} = 1\%$. In this work, we consider that the target PDR is 99%. In order to take the impact of interference from surrounding unlicensed systems into account, we introduce a parameter of interference error rate (IER), which is defined as the probability for each packet to be lost due to interference. We fix IER over 5 GHz to be 5% while we vary IER over 2.4 GHz considering that more number of unlicensed devices exist over 2.4 GHz than 5 GHz, which can lead to highly interfered period. Specifically, for 2.4 GHz, we employ a model based on Gilbert-Eliot model shown in Fig. 4 [15]. We prepare two interference states, Good and Bad, which are transited with probability shown in Fig. 4. The transition of interference state is assumed to occur independently over different channels (i.e., interfaces), where $p = 1\%$ and $r = 10\%$. The IER over Good state is fixed to be 1% while we conduct simulations for different IER over Bad state, defined as IER_B, which is set to 10%, 50%, and 90%.

Table 2. Simulation parameters

Common parameters	Error model	Nist error model
	Tx. Power	20 mW
	Power Consumption in Tx. State	1.99 W [12]
	Power Consumption in Rx. State	1.27 W [12]
	PHY Rate (Mbps)	14.4, 28.9, 43.3, 57.8 86.7, 115.6, 130, 144.4
	Max. Num. Retransmissions	5
STA	Num. of IFs (N_{STA})	2
	Packet Size	1496 Bytes
	Packet Generation Period	0.03 s
	FEC Rate	1/3
	Mobility Model	Random Way Point
	Velocity	15 m/s
	Altitude	15 m
RN	Number of RNs	10
	Num. of IFs (N_{RN})	3
	Position	Random (Uniform)
AP	Num. of IFs (N_{AP})	5
	Position	Center of Area
Channel Model	Path Loss	Coefficient: 2.85 [13]
	Fading	Block Rayleigh (Block Length: 50 ms)

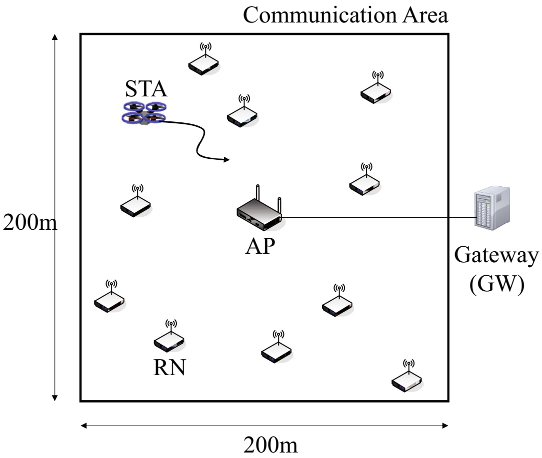

Fig. 3. Simulation model.

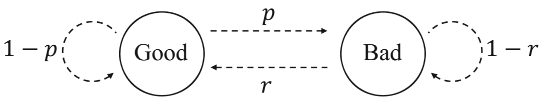

Fig. 4. The employed model for transiting interference states over 2.4 GHz.

We employ the following performance metrics in our evaluations:

- Packet Delivery Ratio (PDR)
  The ratio of number of packets transmitted by STA to that received at GW, all in application level.
- Average Delay
  The average time from packet generation at STA to its arrival at GW. Here, we take the reordering of packets into account, where AP is controlled to wait for the missing packets for at most 50 ms before its forwarding to GW. For simplicity, we neglect the delay for packet forwarding from AP to GW.
- Fractional Airtime of RN
  The ratio of total channel occupancy period of all RNs to total simulation period.
- Maximum RN Energy Consumption
  The maximum energy consumption of RN among all RNs.
- Fractional Airtime of STA
  The ratio of total channel occupancy period of STA to total simulation period.

As for reference schemes, we consider single–link broadcast (SL–BC), where a single IF is employed for data transfer by STA (i.e., $N_{STA} = 1$), where FEC rate of 1/3 is employed. Furthermore, we also consider multi–link unicast (ML–UC), where multi–link transmissions with $N_{STA} = 2$ are employed by STA with each IF connected to a reception point by using unicast mode. Each IF at STA with ML–UC employs PHY rate adaptation based on ARF as well as handover control to switch its reception point. In the handover control, each IF at STA observes RSSIs of beacons transmitted by each reception point, which includes IFs at AP and all RNs, every 1 s, and calculates its averaged value. Then, if IF at STA detects better reception point, which offers higher average RSSI by 3 [dB] than its current link, it switches its reception point to the corresponding new point. On the other hand, we call the multi–link and multi–relay broadcast transmissions described in Sect. 2 as ML–BC. For FEC in ML–BC, different set of redundant packets are assumed to be transmitted by STA over each IF.

5.2 Simulation Results

First, in order to investigate the gain brought by multi–link and multi–relay transmissions, we compare performance of SL–BC and ML–BC, and those with and without RNs. Figures 5 and 6 respectively show PDR and average delay against different PHY rates employed by STA, where IER_B is set to 90%. Here, STA is supposed to employ a fixed rate depicted in horizontal axis in Figs. 5 and 6 for whole simulation period. First, from Fig. 5, we can see that the gain brought by introducing RNs is larger for higher PHY rates. With higher PHY rates, the communication range of STA becomes smaller, which results in higher probability for STA to be located outside the communication range of AP. However, with the existence of RNs, STA can deliver data to AP through surrounding RNs even with higher PHY rates. That is why the benefit to utilize RN is larger for higher PHY rates. Next, Fig. 5 shows that ML–BC has better PDR than SL–BC. This is thanks to channel diversity, where packets lost over one interface due to interference can be received over the other interface with ML–BC. From Fig. 5, it can be seen that the target PDR of 99% can be achieved by ML–BC with RN when PHY rates equal to or less than 43.3 Mbps are employed by STA. The same tendency is observed for average delay as shown in Fig. 6, where smaller delay is achieved for higher PDR. For ML–BC with RN employing PHY rates equal to or less than 43.3 Mbps, PDR is sufficiently high, therefore, the average delay becomes smaller as PHY rate is increased. In summary, these two figures show the effectiveness of multi–link and multi–relay transmissions of ML–BC.

Next, we analyze the impact of OH and proposed rate control on achievable performance of ML–BC. Here, when we employ a fixed PHY rate for ML–BC (i.e., when we do not employ the proposed rate control), we adopt 43.3 Mbps based on the above results on PDR and average delay. Figures 7 and 8 respectively show fractional airtime of RN and maximum RN energy consumption against IER_B for ML–BC employing a fixed rate with and without OH, and ML–BC employing the proposed rate control with OH. In these evaluations, we confirmed that all three schemes achieve PDR higher than the target value of 99% for IER_B given in the figures. First, from Fig. 7, we can see that ML–BC with fixed rate can decrease fractional airtime of RN by introducing OH, which means that the suppression of redundant packets properly works at each RN. However, Fig. 8 shows that the introduction of OH into ML–BC with fixed rate does not provide gain in terms of RN energy consumption. This is because,

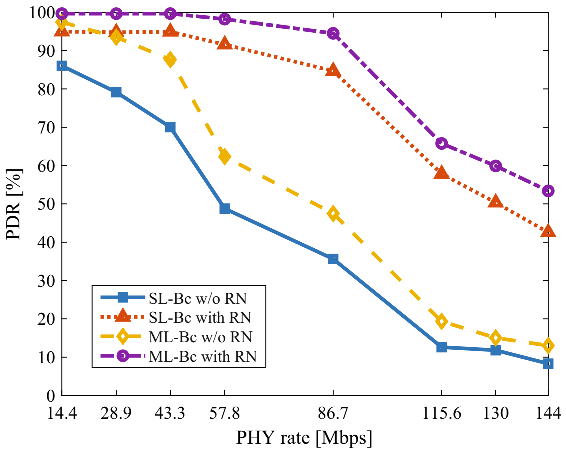

Fig. 5. PDR against different PHY rates employed by STA for SL–BC and ML–BC with and without RN ($IER_B = 90\%$).

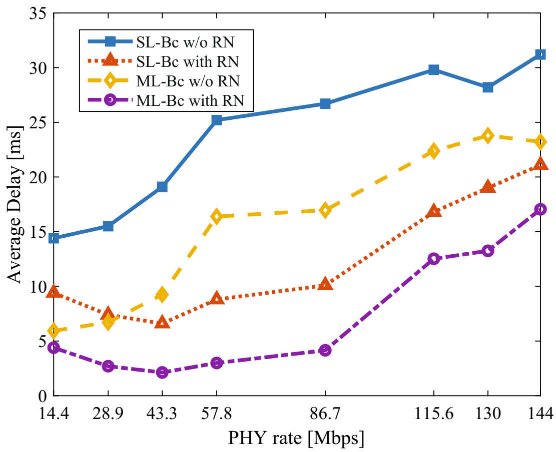

Fig. 6. Average Delay against different PHY rates employed by STA for SL–BC and ML–BC with and without RN ($IER_B = 90\%$).

while the energy consumed for transmissions of redundant packets is successfully reduced by OH, the additional energy is required with OH for each RN to observe any packet transmitted by the other RNs. However, we can see an interesting observation in these figures that we can achieve minimum airtime and energy consumption of RN by jointly applying OH and proposed rate control to ML–BC. The proposed rate control adjusts PHY rate of STA in such a way that minimum number of required RNs successfully decode packets transmitted by STA. This enables only RNs located closely to STA to successfully decode the transmitted packets, which contributes to limit the number of RNs involved into OH operations, and additionally, reduces the distance among RNs which attempts to mutually overhear the forwarded packets. This leads to the improvement of probability to successfully overhear each packet forwarded by a small number of RNs within the proximity of STA, thereby reducing the energy consumed by RN with ML–BC jointly employing OH and proposed rate control. From these results, we can confirm the effectiveness of our proposed rate control.

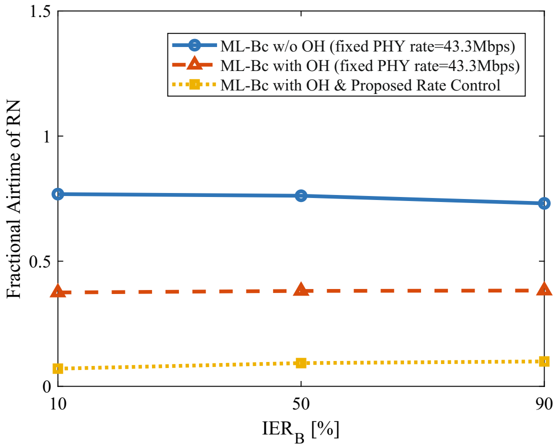

Fig. 7. Fractional airtime of RN against IER_B for ML–BC employing a fixed rate with and without OH and ML–BC employing the proposed rate control with OH.

Finally, we compare performance of ML–BC and ML–UC in order to clarify the benefit brought by broadcast mode employed at STA. Figure 9 shows PDR against IER_B while Figs. 10 and 11 respectively show fractional airtime of IF1 and IF2 at STA for ML–UC and ML–BC employing the proposed rate control and OH. Figure 9 shows that ML–BC realizes reliable data transmissions for any value of IER_B. On the other hand, ML–UC cannot offer PDR higher than the target value of 99% even for $IER_B = 10\%$, which degrades more for larger IER_B. This is due to the failure of handover and rate control for unicast mode, caused by high mobility of drone (i.e., STA). The switch of a reception point as well as employed rate cannot adapt to the rapid variation of link condition with ML–UC, which often causes continuous packet losses exceeding the maximum number of link–level retransmissions, thereby degrading PDR. Furthermore, the increased number of retransmissions of ML–UC results in larger fractional airtime as shown in Figs. 10 and 11, which deteriorates more as IER_B is increased. On the other hand, handover control is unnecessary for ML–BC, which enables STA to transmit data to surrounding reception points seamlessly. Furthermore, the proposed rate control allows STA to promptly change its PHY rate to a

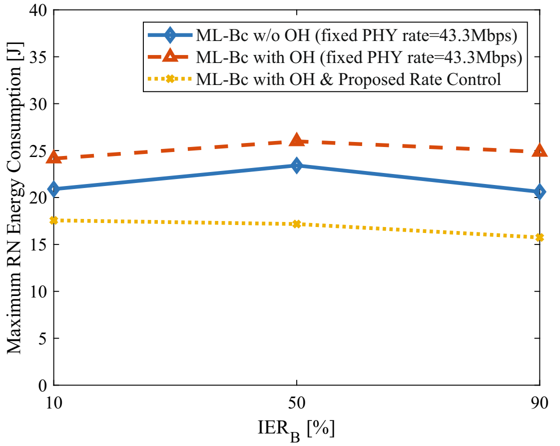

Fig. 8. Maximum RN energy consumption against IER_B for ML–BC employing a fixed rate with and without OH and ML–BC employing the proposed rate control with OH.

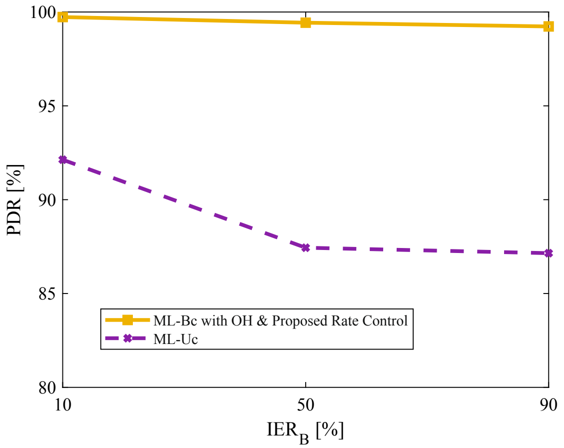

Fig. 9. PDR against IER_B for ML–BC employing the proposed rate control with OH and ML–UC.

proper value at a given location. Thanks to these advantages, ML–BC achieves higher PDR than ML–UC while achieving much smaller fractional airtime of STA than ML–UC. These results confirm the superiority of ML–BC to ML–UC.

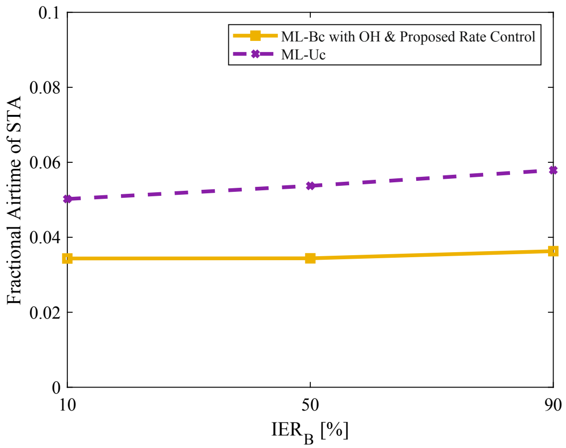

Fig. 10. Fractional Airtime of IF1 at STA against IER_B for ML–BC employing the proposed rate control with OH and ML–UC.

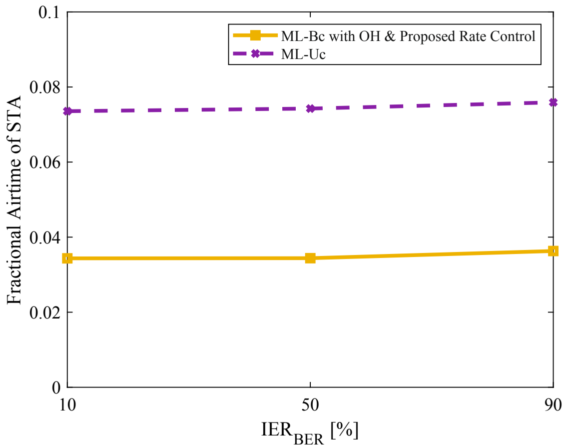

Fig. 11. Fractional Airtime of IF2 at STA against IER_B for ML–BC employing the proposed rate control with OH and ML–UC.

6 Conclusions

In this paper, we focused on real–time data transmissions from a drone supported by wireless LAN. In order to enhance the reliability, we introduced a multi–link and multi–relay system integrated with broadcast transmissions employing packet–level forward error correction. We first confirmed the effectiveness and practicality of the multi–link and multi–relay system supporting data transmissions from a drone by experiments. Then, we enhanced the multi–link and multi–relay system by proposing rate control for STA to dynamically set its physical layer (PHY) rate based on its position and the link quality for surrounding relays. We also applied overhearing function to each relay to prevent redundant forwarding of the same packets by multiple relays. With computer simulations, we extensively study packet delivery rate, delay, channel occupancy period, and energy consumption of each relay. Our simulation results showed that the multi–link and multi–relay system improves energy efficiency of relays when the proposed rate control and overhearing are jointly employed. Furthermore, we showed that the multi–link and multi–relay system with link–level broadcast enjoys channel and route diversity, and has superior performance to a common unicast based system.

Our future work includes experimental studies with the implementation of proposed rate control and overhearing functions into our testbed, considering the practical issues, such as GPS errors. Dynamic FEC control is also an interesting future work.

References

1. Wang, X., Chowdhery, A., Chiang, M.: SkyEyes: adaptive video streaming from UAVs. In: Proceedings of the 3rd Workshop on Hot Topics in Wireless, October 2016
2. Xiao, X., Wang, W., Chen, T., Cao, Y., Jiang, T., Zhang, Q.: Sensor-augmented neural adaptive bitrate video streaming on UAVs. IEEE Trans. Multimedia **22**, 1567–1576 (2019)
3. He, S., Wang, W., Yang, H., Cao, Y., Jiang, T., Zhang, Q.: State-aware rate adaptation for UAVs by incorporating on-board sensors. IEEE Trans. Veh. Technol. **69**(1), 488–496 (2020)
4. Ikeda, K., Imai, Y., Yomo, H., Kondo, Y., Yokoyama, H.: Data transmissions from a drone using multi-AP wireless LAN: a field trial. In: 2020 29th International Conference on Computer Communications and Networks (ICCCN) (2020)
5. Katila, C.J., Di Gianni, A., Buratti, C., Verdone, R.: Routing protocols for video surveillance drones in IEEE 802.11s wireless mesh networks. In: 2017 European Conference on Networks and Communications (EuCNC) (2017)
6. Matsuda, T., Noguchi, T., Takine, T.: Broadcasting with randomized network coding in dense wireless ad hoc networks. IEICE Trans. Commun. **E91-B**(10), 3216–3225, October 2008
7. Kamerman, A., Monteban, L.: WaveLAN-II: a high-performance wireless LAN for the unlicensed band. Bell Labs Tech. J. **2**, 118–133 (1997)
8. Japan UAS Industrial Development Association (JUIDA). https://uas-japan.org/en/
9. DJI phantom 4. http://www.dji.com/product/phantom-4
10. Song, W., Ju, P., Jin, A.L., Cheng, Y.: Distributed opportunistic two-hop relaying with backoff-based contention among spatially random relays. IEEE Trans. Veh. Technol. **64**(5), 2023–2036 (2015)
11. Pei, G., Henderson, T.R.: Validation of OFDM error rate model in NS-3. Boeing Research & Technology, Technical report (2010)
12. Halperin, D., Greenstein, B., Sheth, A., Wetherall, D.: Demystifying 802.11n power consumption. In: Proceedings of the 2010 International Conference on Power Aware Computing and Systems, HotPower 2010, p. 1. USENIX Association, USA (2010)

13. Zhou, T., Sharif, H., Hempel, M., Mahasukhon, P., Wang, W., Ma, T.: A deterministic approach to evaluate path loss exponents in large-scale outdoor 802.11 WLANs. In: 2009 IEEE 34th Conference on Local Computer Networks, pp. 348–351 (2009)
14. Saeed, A., Khan, L., Shah, N., Ali, H.: Performance comparison of two anycast based reactive routing protocols for mobile ad hoc networks. In: 2009 2nd International Conference on Computer, Control and Communication, pp. 1–6 (2009)
15. Bildea, A., Alphand, O., Rousseau, F., Duda, A.: Link quality estimation with the Gilbert-Elliot model for wireless sensor networks. In: 2015 IEEE 26th Annual International Symposium on Personal, Indoor, and Mobile Radio Communications (PIMRC), pp. 2049–2054 (2015)